# 1 Dynamic techniques for the rejection of the offset and low frequency noise

## 1.1 Motivations.

The accuracy and resolution of an acquisition system is significantly degraded at DC and low frequencies by the presence of offset, offset drift and flicker noise. This problem has been known since the development of the first DC amplifiers based on vacuum tubes, designed to read the signals of sensors such as thermocouples and photoelectric cells, characterized by very low signal levels. In order to overcome this limitation, various dynamic solutions have been invented.

The improvement of bipolar technologies and architectures lead to the introduction of instrumentation amplifiers with very low flicker noise densities and low offset. Very popular amplifiers such as the AD620 (Analog Devices™) are marked by offset voltages that approach 10 μV and total peak-to-peak noise at low frequencies (e.g in the 0.1-10 Hz Bandwidth) well below 1 μV.

However, it should be observed that:

1) Frequently, these performances are not sufficient, especially as far as offset and offset drift are concerned.

2) These results require individual trimming of the amplifiers.

3) The performance of CMOS amplifiers is at least one order of magnitude worse, even using exceptionally large device areas to mitigate flicker noise and improve matching.

4) Complex CMOS analog circuit are becoming more and more important for the reduced cost of pure CMOS processes and the easiness of integration with digital circuits to form single chip acquisition systems.

As a result, the adoption of dynamic techniques for offset cancellation and low frequency noise reduction has become mandatory in modern data acquisition systems and continuous research activity is being carried out in this field to obtain more and more performing integrated circuit.

Dynamic offset cancellation techniques can be divided into the following three main categories [1]:

- Auto-Zero (AZ)
- Correlated Double Sampling (CDS)
- Chopper Modulation, indicated also as Chopper Stabilization (CHS).

In the following part of this document, we will indicate the total error voltage referred at the input of an amplifier with the symbol $v_n$ and, unless differently specified, we will consider that also the random offset is included in the $v_n$ stochastic process.

## 1.2 Auto-zero (AZ)

The auto-zero approach is based on a simple idea: if it is possible to measure the offset of an amplifier then it is also possible to save it in an analog or digital memory and subtract it from the signal, obtaining virtually offset-free operation. This simple procedure is indeed used to compensate (calibrate) the offset of various instruments and can even be carried out manually. In order to read the offset of an amplifier it is necessary to disconnect it from the signal and insert a zero signal at the input. For a voltage amplifier, this means to short the input port, while for a current amplifier the input port should be left open.

Unfortunately, the offset is not constant, but varies with time due to the effect of drifts. Therefore, offset calibration should be performed frequently. If we want also to reject low frequency noise contributions, the time between two calibration events gets so short that it is no more feasible to perform it manually.

In the AZ amplifier, the offset is sampled at frequencies that reach several kHz, so that the resulting technique should be regarded as a real dynamic offset cancellation approach.

Figure 1.1 schematically shows the two phases of an AZ amplifier, applied to a voltage amplifier. Let us consider that the amplifier characteristic is given by:

$$v_{out} = A\left(v_{in} - v_n\right) \tag{1.1}$$

1. In the Auto-Zero phase, the input is shorted to ground, so that $v_{in}$=0, thus $v_{out}$= $-Av_n$. The output noise voltage (including offset) is sampled at a certain instant $t_c$ during the AZ phase and stored into a memory element.
2. After the AZ phase, the amplifier gets into the normal operation phase, where the stored output offset voltage is subtracted from the output signal.

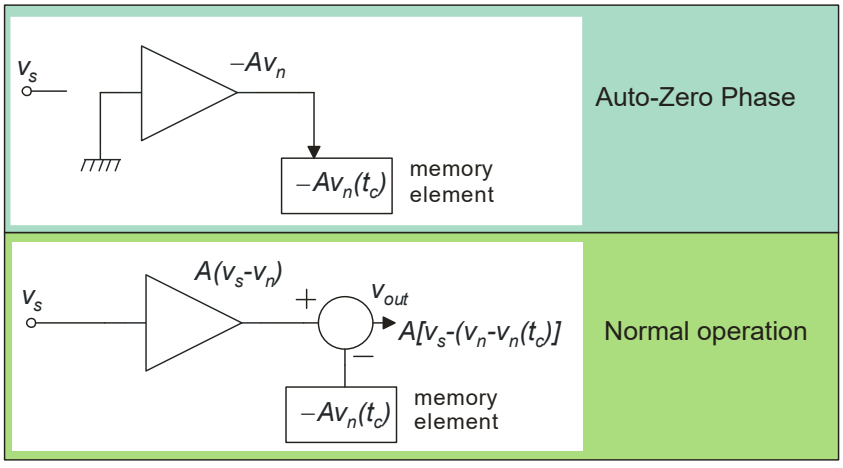


Fig. 1.1. Schematic representation of the auto-zero operating principle

The resulting output signal is given by:

$$v_{out} = A\left(v_s(t) - v_n(t) + v_n(t_c)\right) \tag{1.2}$$

In order to cancel also variable components of $v_n$, the AZ phase is periodically repeated at a frequency $f_{ck}$ (clock frequency). The corresponding timing diagram is shown in Fig.1.2, where the AZ phase occurs when the clock is low. The target is to make the amplifier work as much as possible as a normal time-continuous amplifier. For this reason the auto-zero phase is made much shorter than the normal operation phase. If we indicate the repetition period with $T=1/f_{ck}$, then we require that

$$t_{AZ} << T \tag{1.3}$$

As far as the output waveform is concerned, a discontinuity occurs across any AZ phase since the stored noise value is updated and a step equal to the difference between the old and new noise value is applied. During the AZ phase, the output signal either go to zero, as in Fig.1.2, or is held by a track-and-hold circuit. Since the AZ phase is generally so short to be considered instantaneous ($t_{az} \rightarrow 0$), the behavior of the amplifier during the AZ phase can be neglected. Thus, as far as the input signal is considered, application of the AZ technique does not alter the original time-continuous response of the amplifier. In this condition, according to (1.2), the effective residual noise is given by:

$$v_{n-eff} = \left(v_n(t) - v_n(nT)\right) \tag{1.4}$$

where $n$ is an integer index and the AZ phase (and offset sampling) occurs at instants ($nT$).

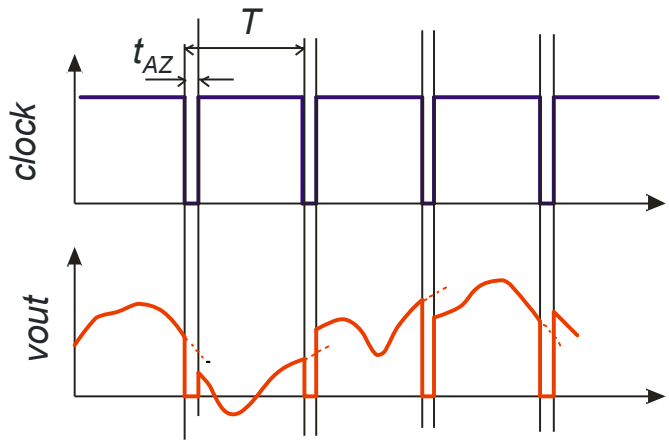


Fig. 1.2. Simplified output waveform of an auto-zero amplifier

Clearly, if $v_n$ is a constant voltage (only the offset component is considered), a perfect cancellation is performed. A satisfactory cancellation will occur also for all those noise contributions that can be considered practically constant across a clock period, where they do not significantly differ from the value sampled in the previous AZ phase. This condition is satisfied by noise spectral components at frequencies much smaller than $f_{ck}$. On the contrary, for $f > f_{ck}$, the noise components can get substantially different than the last sampled value, i.e. $v_n(nT)$, and the difference in Eq.(1.4) is not zeroed.

In order to obtain a useful expression of the residual noise of the amplifier, it is necessary to calculate the spectral density of $v_{n\_eff}$. The procedure is illustrated in Fig.1.3. Let us consider a single occurence (i.e. a single signal) of the stochastic process, and indicate it with $v_n(t)$. In this case, $v_n(t)$ can be considered as a deterministic signal and can be represented, at least for now, by its Fourier transform (spectrum). The $v_n$ spectrum is represented on the top left of Fig.1.3. On the right, we graphically show how the spectrum of $v_n(nT)$ can be obtained. This is the result of sampling $v_n(t)$ and maintaining it (sample and hold) across all the clock period. The spectrum will then be given by:

$$v_n(nT) \rightarrow e^{-j\pi fT}\operatorname{sinc}(\pi fT)\left[\sum_{k=-\infty}^{\infty} V_n(f - kf_{ck})\right] \tag{1.5}$$

where sinc($x$)=sin($x$)/$x$ and $V_n(f)$ is the spectrum of $v_n(t)$. Expression (1.5) means that we have to add an infinite number of replicas of $V_n(f)$, shifted by multiples of $f_{ck}$, and then multiply the result of this sum by a sinc function. Considering the difference in Eq.(1.4), the spectrum of the residual noise $v_{n\text{-}eff}$ is given by:

$$V_{n-eff}(f) = V_n(f) - e^{-j\pi fT}\operatorname{sinc}(\pi fT)\left[\sum_{k=-\infty}^{\infty} V_n(f - kf_{ck})\right] \tag{1.6}$$

Combining the 0-order replica (that is the replica with $k$=0, which is not shifted along the frequency axis) with the $V_n(f)$ spectrum, the following compact expression can be found.

$$V_{n-eff}(f) = \sum_{k=-\infty}^{\infty} H_k(f) V_n(f - kf_{ck}) \tag{1.7}$$

where:

$$\begin{cases} H_0(f) = 1 - e^{-j\pi fT}\operatorname{sinc}(\pi fT) \\ H_k(f) = -e^{-j\pi fT}\operatorname{sinc}(\pi fT) \end{cases} \tag{1.8}$$

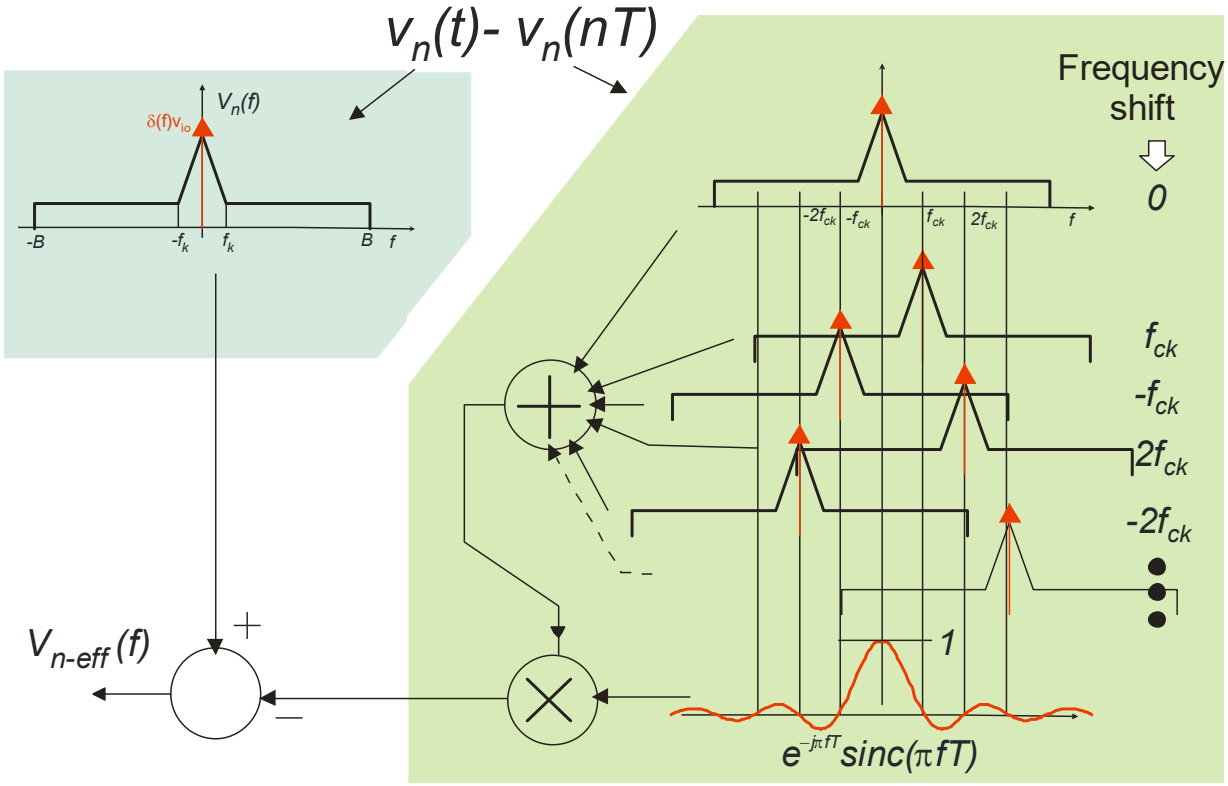


Fig. 1.3. Operation performed on the single signal by the auto-zero amplifier in the frequency domain

Note that:

1. The spectrum of $v_n(t)$ is partially cancelled by the 0-order (not shifted) replica contained in the sum. The cancellation occurs only at low frequencies, where the sinc function is practically equal to one.
2. According to (1.7), the time domain operation applied to the noise is equivalent to (i) modulating the noise itself by sinusoidal signals with frequencies multiples of $f_{ck}$; (ii) filtering the results of the modulation by filters $H_k(f)$; (iii) summing up all the components created in this way. Since modulating the original stochastic process with different modulation frequencies produces uncorrelated processes, and filtering does not alter this condition, we can obtain the power spectral density of the resulting process by simply summing up the spectral densities of each individual component. Therefore:

$$S_{vn-eff}(f) = \sum_{k=-\infty}^{\infty} |H_k(f)|^2 S_{vn}(f - kf_{ck}) \tag{1.9}$$

where $S_{vn}$ is the power spectral density of the amplifier noise $v_n$.

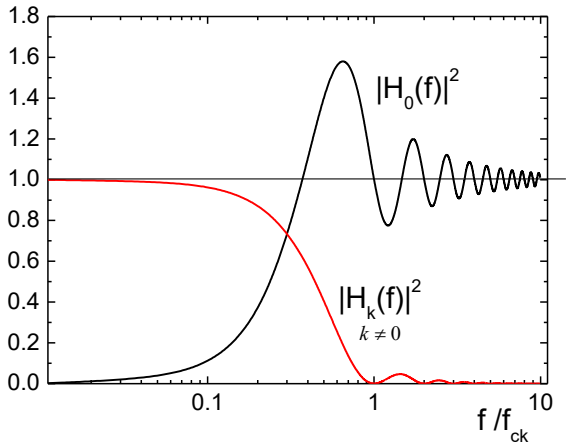


Fig. 1.4. Frequency response of functions $|H_0(f)|^2$ and $|H_k(f)|^2$

The behavior of the transfer functions $|H_k(f)|^2$ is shown in Fig.1.4. Function $|H_0(f)|^2$ multiplies the 0-order replica of the spectral density, which coincides with the original input noise spectral density of the amplifier. Since $|H_0(f)|^2$ is zero for $f$=0 and stays close to zero for $f<<f_{ck}$, the amplifier offset and low frequency noise components are cancelled or strongly reduced. If $f_{ck}>f_k$, where $f_k$ is the corner frequency of the flicker noise, we can state that the flicker noise is practically cancelled from the 0-order replica. For frequencies $f>>f_{ck}$, $|H_0(f)|^2$ tends to one, and this means that, for these frequencies, the amplifier power spectral density is left unchanged. Now we have to consider the contribution of all the other replicas. These replicas are added up and then they are multiplied by $|H_k(f)|^2$, which is practically equal to one around the origin ($f<<f_{ck}$) and rapidly tends to zero for higher frequencies. Therefore, these replicas will affect only the amplifier noise in an interval around the origin, or, more precisely, at frequencies $f<f_{ck}$. In addition, we should consider that a $k$-order replica (that is a replica shifted by $kf_{ck}$) would shift the offset and flicker noise component around the frequency $kf_{ck}$. Fortunately, $|H_k(f)|^2$ is zero for all multiples of $f_{ck}$, so that these contributions are effectively cancelled.

Considering the graphical representation of Fig.1.3 and supposing that $f_{ck}>f_k$, it can be easily understood that the contribution of all replicas (except for the 0-order replica) at $f<<f_{ck}$ is only given by the $S_{BB}$ component. Fig.1.5 shows the contributions of the various replicas, considering only replicas that are shifted towards the positive frequencies. For the reasons expressed above, we are interested only to the contributions in an interval close to the origin. Furthermore, we have not represented the flicker component since, as previously discussed, it gives no significant contribution. Considering the finite bandwidth of the amplifier (and thus, of the noise density), the number of replicas that give a contribution is $B/f_{ck}$. Repeating this operation for the negative shifts, the total contribution around the origin is:

$$S_{vn-eff}(f) \cong \frac{2B}{f_{ck}} S_{BB} \quad \text{for } f < f_{ck} \tag{1.10}$$

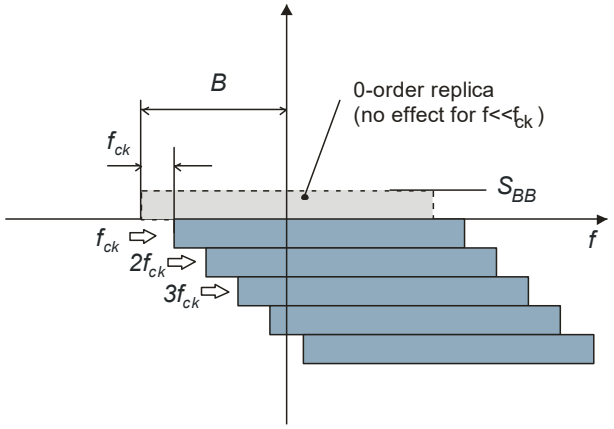


Fig. 1.5. Illustration of the fold-over mechanism

A simplified picture of the resulting spectral density is shown in Fig.1.6 and can be summarized in the following way:

1) In the frequency interval from DC to roughly $f_{ck}$: the flicker noise and offset are no more present, but they are substituted by an almost flat spectral density equal to $2B/f_{ck}$ times $S_{BB}$. This phenomenon, which is due to aliasing of the noise density replicas, is called "noise foldover" or "noise-foldback".
2) At frequencies $f>f_{ck}$, only the 0-order replica, weighted by $|H_0(f)|^2$ is present. Due to the behavior of $|H_0(f)|^2$ , the resulting noise density is similar to that of the original amplifier, apart from some oscillations (see Fig.1.4), which we have neglected in Fig.1.6.

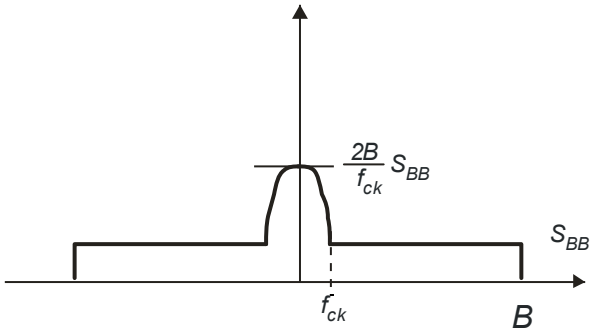


Fig. 1.6. Simplified residual noise of an auto-zero amplifier

## 1.3 Correlated Double Sampling (CDS)

The CDS technique differs from the AZ in the fact that also the signal, and not only the noise, is sampled. Since we cannot sample the signal without sampling also the noise/offset (otherwise we would not need offset cancellation techniques at all!), the noise/offset is sampled two times. In particular, the CDS is composed of two phases:

Phase 1: The signal is removed from the input of the system, so that only the offset is present. The offset is sampled (first sample).

Phase 2: The signal is connected at the input of the system and the result is sampled (second sample). Obviously, this second sample includes both the signal and the offset/noise. The difference between the first and second sample is the output of CDS.

Note that phase 1 is identical to the first phase of the AZ technique. The difference is that, in the following phase, the AZ amplifier behaves like a time continuous system, while, in the CDS, this never happens and the result will be available only at the end of the second phase, when the second sample is taken. A system that uses CDS for offset cancellation should be considered a real sampled data system.

The expression of the CDS output is then given by the following expression:

$$v_{out}(nT) = A\left[v_s(nT) - v_n(nT) + v_n(nT - t_R)\right] \tag{1.11}$$

where $t_R$ is the time lapse from the first and second sample. As for the AZ, we will indicate both the noise and offset component with $v_n$, and we will refer to both with simply the term "noise". Note that both the noise and the output signal are treated as discrete time functions, produced by sampling the corresponding time continuous functions.

The result of CDS is that all noise components that remain practically constant across the time lapse $t_R$ give the same contribution to the two noise samples and then are cancelled. The contributions that do not change significantly across the two samples can be considered "correlated". The fact that the CDS technique is effective for noise components that are correlated across the given time lapse inspired the adjective "correlated" for the technique.

Very often $t_R$ is half the clock period, that is $t_R=T/2$. By this consideration, the residual noise is given by:

$$v_{n-eff}(nT) = v_n(nT) - v_n(nT - \frac{T}{2}) \tag{1.12}$$

It is important do calculate the DPSD (Discrete Power Spectral Density) of $v_{n\text{-}eff}(nT)$. To do this, we can refer to the model shown in Fig.1.7, valid only for the noise components.

The transfer function (in the Fourier domain) from $v_n$ to the time continuous signal $v_{tc}$, is given by:

$$H(f) = \frac{V_{tc}(f)}{V_n(f)} = 1 - e^{-j2\pi f\frac{T}{2}} = e^{-j\pi f\frac{T}{2}}\left(e^{j\pi f\frac{T}{2}} - e^{-j\pi f\frac{T}{2}}\right) = e^{-j\pi f\frac{T}{2}} \cdot 2j\sin\left(\pi f\frac{T}{2}\right) \tag{1.13}$$

Then, considering that $v_n(t)$ is a stochastic process of power spectral density (PSD) $S_{vn}(f)$, the PSD of $v_{tc}(t)$ will be:

$$S_{vtc}(f) = \left|H(f)\right|^2 S_{vn}(f) = 4\sin^2\left(\pi f\frac{T}{2}\right)S_{vn}(f) \tag{1.14}$$

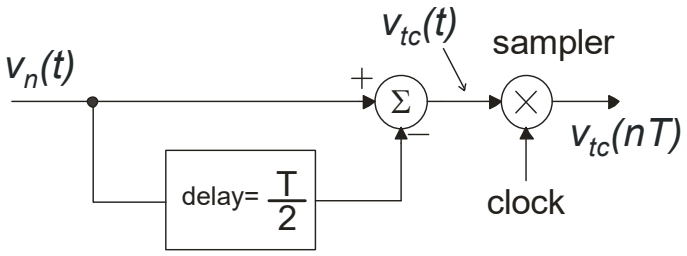


Fig. 1.7. Equivalent block diagram valid only to determine the effective noise.

The effect is weighting the original power spectrum by a $\sin^2$ function, as shown in Fig.1.8.. The desirable effect is the cancellation of the offset component and the strong reduction of the low frequency noise contributions. If $f_{ck} >> f_k$, then a complete flicker noise cancellation can be assumed.

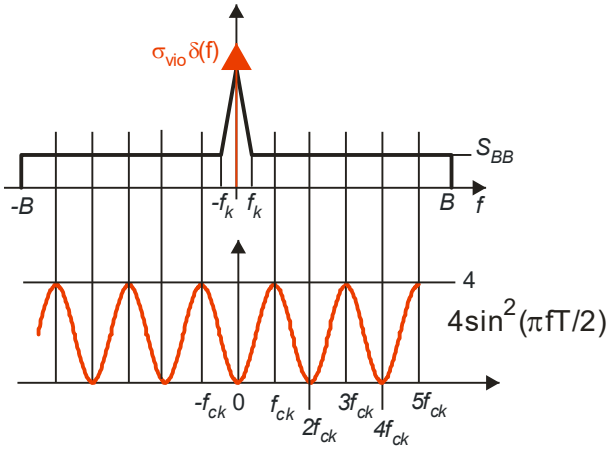


Fig. 1.8. Multiplication of the original amplifier noise PSD (top) by function $|H(f)|^2$, (bottom) gives the PSD of *Vtc*.

The final discrete time noise sequence, $v_{n\text{-}eff}(nT)$ is obtained by sampling the $v_{tc}(t)$ noise. As a result, replicas of the $S_{vtc}(f)$ PSD are produced and summed up to form the $S_{vn\text{-}eff}(f)$ DPSD. Since we are dealing with discrete time signals, we are interested only to the result of this sum in the interval $[-f_{ck}/2, f_{ck}/2]$. For the reasons expressed above, we can consider that the power spectral density of $V_{tc}$ is practically equal to:

$$S_{vtc}(f) = \begin{cases} 4\sin^2\left(\pi f \frac{T}{2}\right) S_{BB}(f) & \text{for } -B < f < B \\ 0 & \text{for } f \le -B \text{ or or } f \ge B \end{cases} \qquad (1.15)$$

In addition, consider the following property of $\sin^2$, when a shift by an even or odd multiple of $f_{ck}$ is applied:

$$\text{even order}: \quad \sin^2\left[\pi\left(f-2kf_{ck}\right)\frac{T}{2}\right]=\sin^2\left(\pi f\frac{T}{2}-k\pi\right)=\sin^2\left(\pi f\frac{T}{2}\right)$$
$$\text{odd order}: \quad \sin^2\left[\pi\left(f-(2k+1)f_{ck}\right)\frac{T}{2}\right]=\sin^2\left(\pi f\frac{T}{2}-k\pi-\frac{\pi}{2}\right)=\cos^2\left(\pi f\frac{T}{2}\right) \qquad (1.16)$$

This property is graphically shown in Fig.1.9. Combining two replicas obtained by an even shift and an odd shift gives a $4S_{BB}\sin^2+4S_{BB}\cos^2$ term, which becomes frequency independent and equal to $4S_{BB}$. As in the AZ the total number of replicas that gives a contribution at low frequencies is $2B/f_{ck}$. Since in the CDS every couple of replicas (odd+even) gives the contribution $4S_{BB}$, the final DPSD will be:

$$S_{vn-eff}(f)=4\frac{B}{f_{ck}}S_{BB} \qquad (1.17)$$

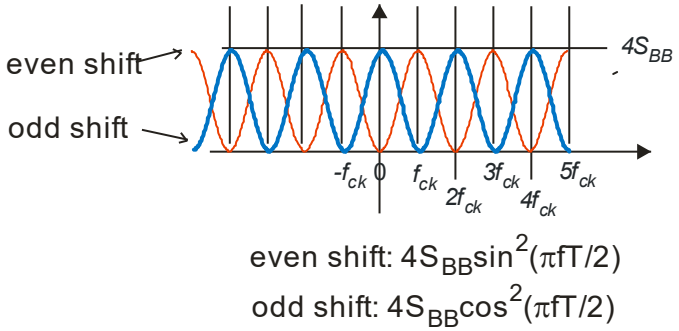


Fig. 1.9. Replicas generated by the final sampling of $v_{tc}$, producing the effective noise $v_{n\text{-}eff}$

## 1.4 Chopper Modulation (CHS).

Modulation can be used to obtain a virtually offset-free amplifier. The scheme is shown in Fig.1.10. The signal, including DC components, is shifted to higher frequencies by means of multiplication by a sinusoidal signal. At this point, it can be processed by the amplifier "A" in a frequency interval that does not include DC and flicker noise.

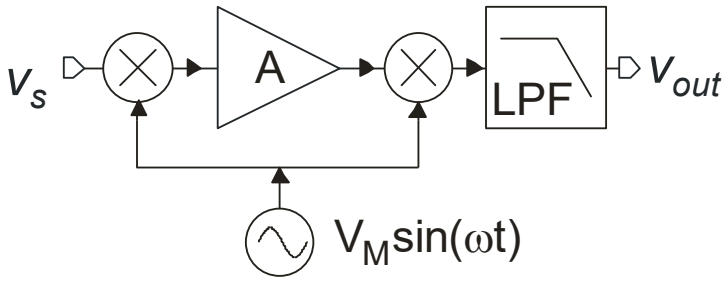


Fig. 1.10. Possible modulation approach base on sinusoidal function (not practical).

Demodulation is operated on the amplified signal by multiplication by the same sinusoidal signal. The demodulator (second multiplication) shits the offset and flicker noise of the amplifier to high

frequencies, where it is suppressed by the low pass filter (LPF). To improve offset cancellation, the amplifier can be an AC coupled amplifier.

This technique is not suitable to be implemented in the form proposed in Fig.1.10. The main problem is the modulator: analog multipliers (e.g. Gilbert cells) are blocks that introduce additional offset and noise. They are suitable for being placed at the output of the amplifier, where the signals are larger and their offset and noise contributions can be neglected, but completely unsuitable to be placed at the input.

In order to overcome these limitations, the sinusoidal modulating and demodulating signal is replaced by a square waveform, as shown in the block diagram of Fig.1.11. This kind of modulation is called "chopper modulation". The advantage is that chopper modulation can be obtained using only switches, which add minimal noise and offset. Amplifiers that incorporate chopper modulation are called "chopper amplifiers" or "CHopper Stabilized amplifiers" (CHS). The term "stabilized" derives from the fact that chopper modulation, like CDS and AZ, eliminates offset and also offset temperature drifts. Indeed, the latter generate output voltage variations that reflect local temperature fluctuations, giving the impression that the amplifier is not stable. Application of CHS stops this output signal "wandering", so that it was originally seen as a sort of "stabilization". Examples of circuits that perform chopper modulation will be described later. Here, we will analyze the effect of chopper modulation on signal and noise. The action of switch-based chopper modulators is equivalent to multiplying the signal by a dimensionless square-waveform of unity amplitude, indicated with $m(t)$ in Fig.1.11.

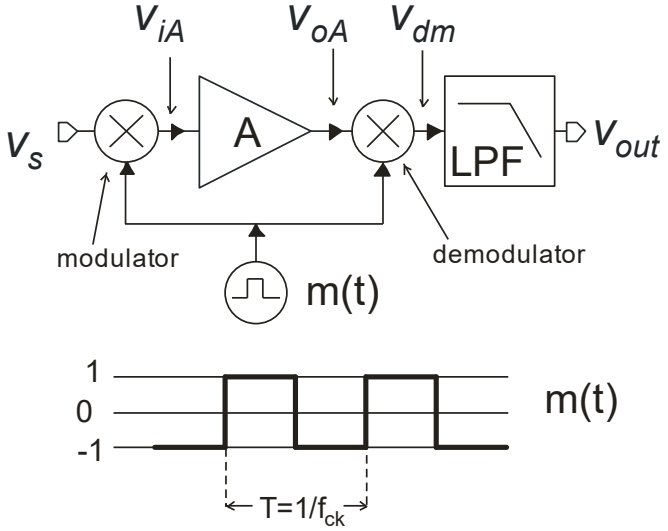


Fig. 1.11. Block diagram of a chopper amplifier (top) and m(t) dimensionless square waveform (bottom)

To understand the operation of the scheme of Fig.1.11, we start by considering a constant input signal. As a first approximation, we will suppose that the amplifier has an infinite bandwidth, so that its transfer function is simply a multiplication by the gain $A$. The output of the amplifier, indicated with $V_{oA}$, is a square wave of amplitude $AV_s$. The demodulator multiplies this square wave by the same $m(t)$ signal. As Fig.1.12 clearly shows, the result is simply an amplified replica of the signal. It can be easily

demonstrated that, whatever signal we have at the input, the succession of modulation and demodulation does not alter the signal itself, which is then simply amplified.

On the other hand, the input offset voltage of the amplifier is not modulated by the input modulator: it appears at the output of the amplifier, amplified by gain $A$. The amplified offset ($-Av_{io}$) is processed only by the demodulator, which produces a square waveform of amplitude $Av_{io}$ and zero mean value. This square wave deriving from offset modulation (called "offset ripple", "chopper ripple" or "chopped offset") includes only frequency components at $f_{ck}$ or above, where $f_{ck}$ is the frequency of the modulating waveform $m(t)$. The output low pass filter LPF is designed to have a cut-off frequency $f_H<f_{ck}$ in order to reject the offset ripple.

In summary, the signal is modulated and demodulated, while the offset (and noise ) is only processed by the demodulator that shifts it to high frequencies so that it can be rejected by the LPF.

To better understand the transformations operated by the chopper modulation on signal and noise, it is convenient to use the frequency domain representation. The square waveform $m(t)$ can be decomposed into a Fourier series as:

$$m(t)=\sum_{k=-\infty}^{\infty} C_k e^{j2\pi k f_{ck} t} \qquad \text{with} \begin{cases} |C_k| = \dfrac{2}{\pi k} & \text{for odd k values} \\ 0 & \text{for even k values} \end{cases} \tag{1.18}$$

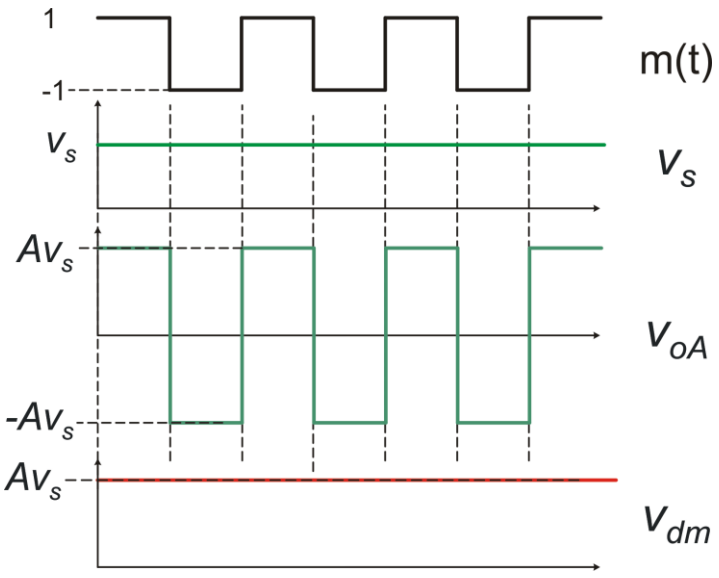


Fig. 1.12. Diagrams illustrating the operations performed on a dc signal by the chopper amplifier

Therefore, the modulator shifts the signal spectrum (Fourier transform) across all odd multiples of frequency $f_{ck}$. The replica shifted at $kf_{ck}$ is multiplied by $C_k$. This process is graphically represented in Fig.1.13. The signal is then amplified by $A$ and finally demodulated. Demodulation consists in shifting again the spectrum by odd multiples of $f_{ck}$ and multiplying the replicas by the corresponding $C_k$ coefficients. Looking at Fig.1.13, it can be easily seen that a replica that was shifted at $kf_{ck}$ by the

modulator, goes back into the baseband (in the original position) by the shift $-kf_{ck}$ applied by the demodulator. In this sequence, the replica is multiplied by $C_kAC_{-k}$. Since:

$$C_{-k} = C_k^* \tag{1.19}$$

then, the spectrum in the baseband at the output of the demodulator is given by:

$$V_{out}(f) = A\sum_{k=-\infty}^{\infty}|C_k|^2 V_s(f) \tag{1.20}$$

The sum of the $|C_k|^2$ is the power of the waveform $m(t)$, which is equal to one. Therefore Eq.(1.20) states the signals is simply amplified by $A$.

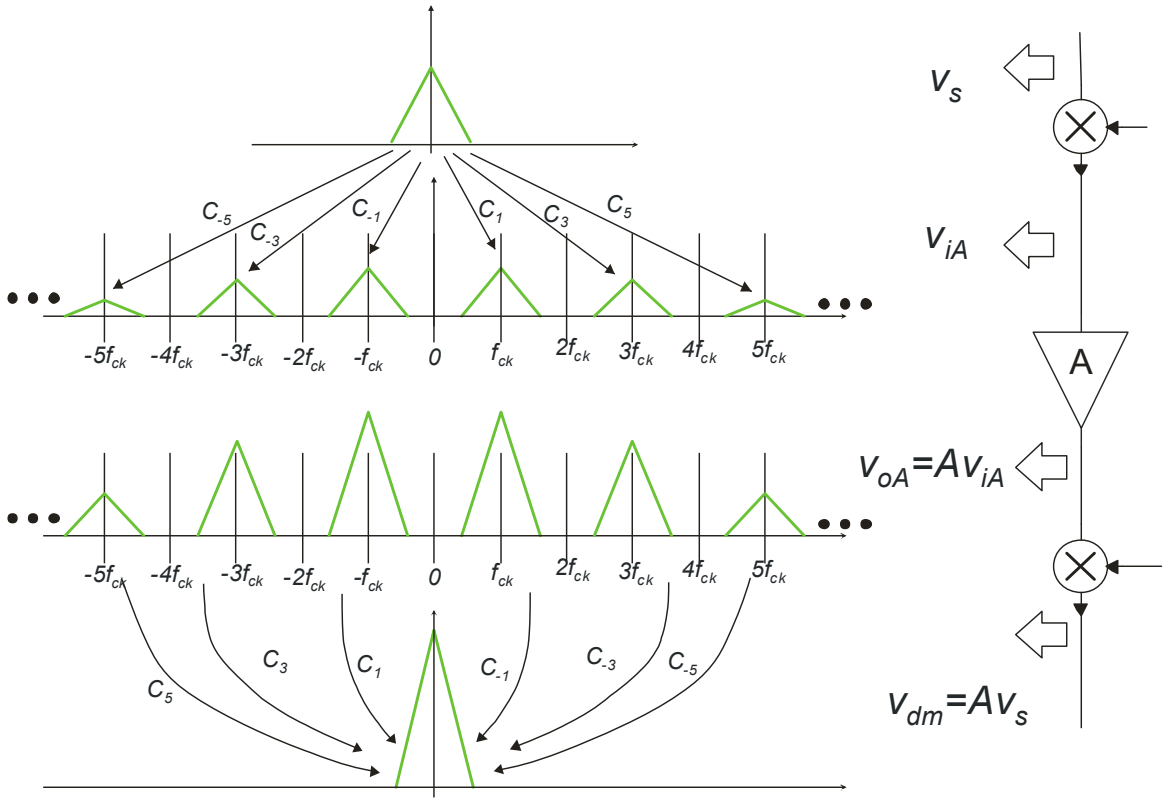


Fig. 1.13. Operations performed on the signal in the frequency domain

Let us consider what happens to the amplifier noise. This is graphically shown in Fig.1.14. The noise power spectral density at the output of the amplifier is shown on top of the figure. This stochastic process is processed by the demodulator, that produces replicas of the noise for each component of the $m(t)$ square waveform spectrum. Note that $m(t)$ has zero mean value, so that the component at zero frequency is also zero. Therefore, there is not a replica with zero frequency shift. For this reason, the offset and flicker noise components do not affect the baseband region. Supposing that $f_{ck} >> f_k$, all replicas give only a baseband contribution proportional to $A^2S_{BB}$. In particular, a replica shifted by $kf_{ck}$ gives a baseband contribution equal to $A^2|C_k|^2S_{BB}$.

As a result, the residual baseband noise is given by:

$$S_{vout}(f) = A^2 \sum_{k=-\infty}^{\infty} |C_k|^2 S_{BB} = A^2 S_{BB} \tag{1.21}$$

Note that Eq.(1.21) gives only the contribution in the baseband, while, at the demodulator output, offset and flicker noise peaks are still present around $f_{ck}$, $3f_{ck}$, $5f_{ck}$, etc. Elimination of these out-of band noise components is the purpose of the LPF, which, as shown in Fig.1.14, limits the bandwidth to frequencies $f<f_{ck}$. It is important to observe that the LPF limits also the signal bandwidth.

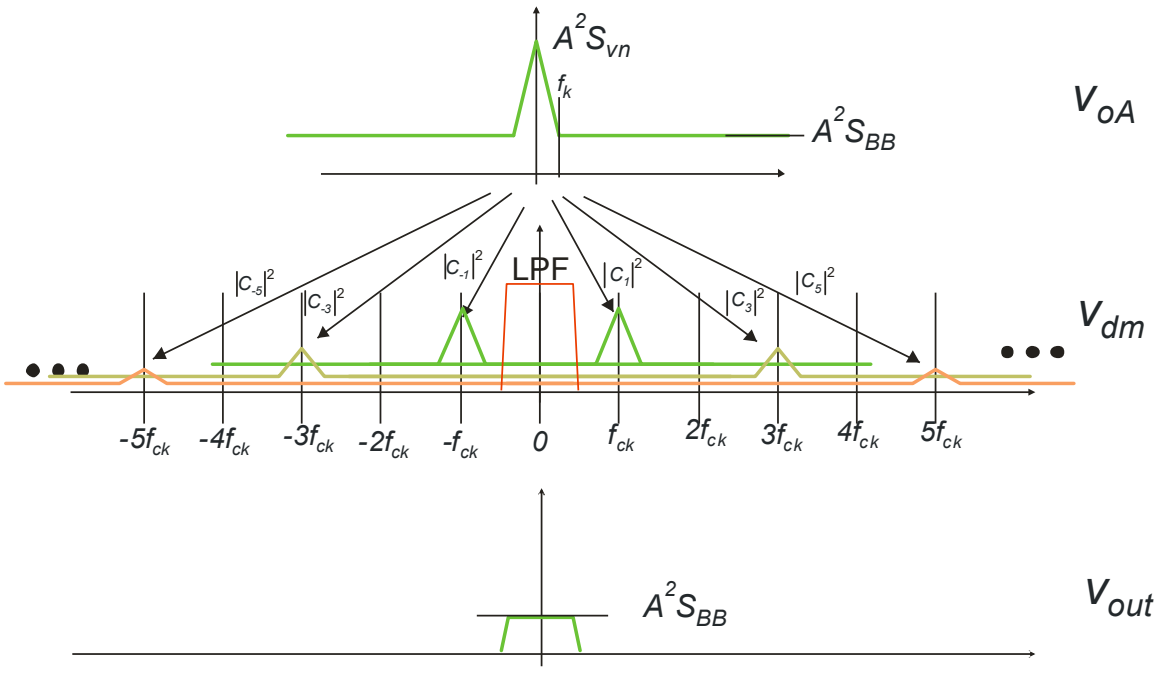


Fig. 1.14. Operations performed on the noise PSD by the chopper amplifier

For most applications, the quantity of interest is not the output noise but the input referred noise. Indicating the input referred noise spectral density with $S_{vn\text{-}eff}$, then $S_{vn\text{-}eff} = S_{out}/A^2$. Therefore:

$$S_{vn-eff}(f) = S_{BB} \tag{1.22}$$

So far, we have considered that the amplifier bandwidth is infinite. This simplifying assumption is clearly not realistic since, in all real cases, the amplifier will be characterized by a finite bandwidth $B$. We will suppose that the amplifier has a low-pass frequency response. As far as the signal is concerned, the amplifier filters the spectrum at the output of the modulator. The result, represented in Fig.1.15, is that replicas at $f>B$ are rejected.

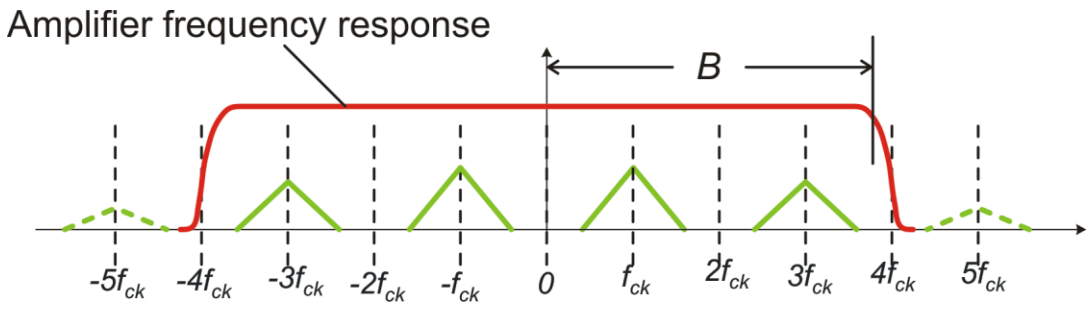


Fig. 1.15. Effect of the finite bandwidth on the signal spectrum

Therefore, the maximum multiple of $f_{ck}$ that gives a replica within the amplifier bandwidth is $B/f_{ck}$. The number of replicas that the demodulator can bring back to baseband is then finite. As a result, Eq. (1.20) becomes:

$$V_{out}(f) = A\left[\sum_{k=-N}^{N}|C_k|^2\right]V_s(f) \qquad \text{with } N = \left\lfloor \frac{B}{f_{ck}} \right\rfloor \tag{1.23}$$

In practice, this means that the actual amplifier gain is given by:

$$A' = \alpha A \qquad \text{with } \alpha = \left[\sum_{k=-N}^{N}|C_k|^2\right] < 1 \tag{1.24}$$

The net effect is then a reduction of the actual amplifier gain. This phenomenon can be understood also in the time domain, if we consider a constant input signal of value $V_S$. Figure 1.16 is analogous to Fig.1.12, but with the hypothesis of infinite amplifier bandwidth removed. The modulator applies a square waveform of amplitude $V_S$ to the amplifier input. Due to the finite bandwidth, the amplifier settles to the final value after a transient, which can be roughly considered $1/B$ long. The result is sketched in Fig.1.16 (signal $V_{oA}$). The demodulator multiplies this signal by $m(t)$, producing the signal $V_{dm}(t)$. Differently form the case of infinite bandwidth (Fig.1.12), this signal is not constant but includes impulses that reach $-AV_S$ and repeat with frequency $2f_{ck}$ . The filter LPF cuts all frequency components for $f>f_H$, where $f_H$ is made smaller than $f_{ck}$, to reject out-of-band noise, as explained earlier. Therefore, $V_{out}$ is constant and equal to the mean value of $V_{dm}$. Due to the negative impulses, the mean value is smaller than $AV_S$, demonstrating that the actual amplifier gain is $A'<A$.

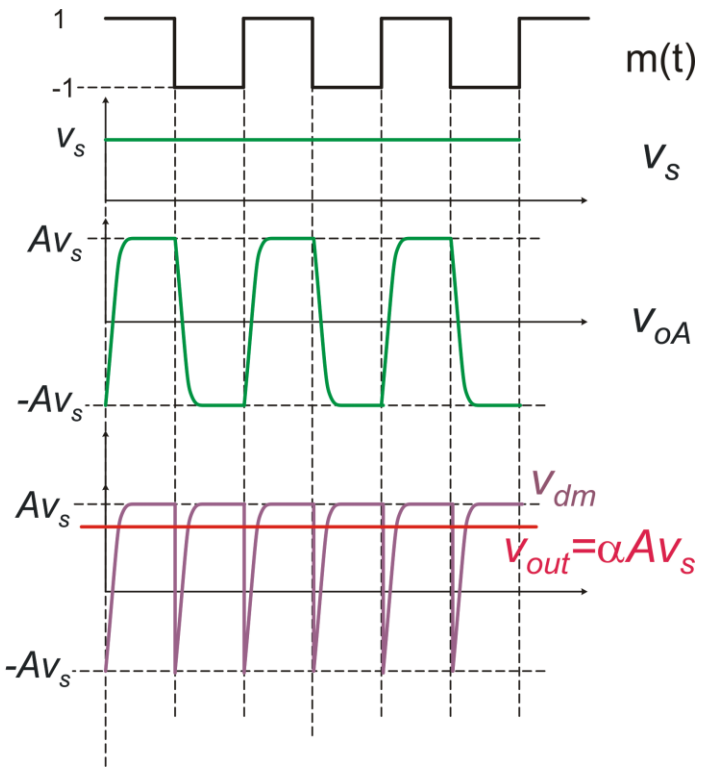


Fig. 1.16. Illustration of the effect of a finite bandwidth in the time domain for an input dc signal

The finite bandwidth of the amplifier slightly affects also the noise. Considering the difference for a case of finite bandwidth is that the noise spectrum $S_{oA}(f)$, taken at the amplifier output port, drops to zero for $f>B$. As a result, replicas with a frequency shift $kf_{ck}>B$ do not give contribution in the baseband. Therefore, also for noise, the maximum $k$ value is $B/f_{ck}$. Equation (1.21) becomes:

$$S_{vout}(f) = A^2 \sum_{k=-N}^{N} |C_k|^2 S_{BB} \qquad \text{with } N = \left\lfloor \frac{B}{f_{ck}} \right\rfloor \tag{1.25}$$

The input referred noise density will be obtained by dividing $S_{vout}$ by the effective gain (squared), which, for a finite bandwidth is $A'=\alpha A$, is given in Eq.(1.24). Then:

$$S_{vn-eff}(f) = \frac{S_{vout}(f)}{\alpha^2 A^2} = \frac{1}{\alpha} S_{BB} \tag{1.26}$$

Since $\alpha<1$, in the case of finite bandwidth the $S_{vn\text{-}eff}$ is slightly higher than $S_{BB}$. This effect is generally considered negligible since, even for the minimum required bandwidth ($f_{ck}=B$), $1/\alpha$ is only equal to 1.23. Therefore $S_{vn\text{-}eff}$ is only 23 % higher than $S_{BB}$. For $B>10\,f_{ck}$ the difference with respect of the ideal case is less than 5%.

An important aspect of the chopper amplifier architecture shown in Fig.1.11 is that the amplifier gain cannot be too large. If the input signal $v_s$, is zero, the signal at the amplifier input ($v_{iA}$ in ) is also zero, so that the amplifier output $V_{oA}$ is equal to $-Av_n$. This signal includes a large constant term, due to the

amplifier offset, and given by $-Av_{io}$. The demodulator transforms it in a zero-mean square waveform (chopper ripple) which is rejected by the LPF. However, it is necessary that $-Av_{io}$ is not too large, otherwise the amplifier output saturates and, when we apply a non-zero input signals, it does not respond to it as required. Even if the amplifier does not saturate, the offset can shift the zero-signal output voltage to a value close to the output range limit, reducing the swing available for the signal. Therefore, the gain of the amplifier should not exceed a maximum value that, for the maximum offset predicted for that amplifier, excessively reduces the signal range. For example, for a maximum input offset of 2 mV and a maximum output swing of 1 V, an amplifier gain of 100 would result in a maximum output offset of 200 mV, producing a 20 % reduction of the available output swing for the signal.

## 1.5 Examples of circuits implementing the offset cancellation techniques.

The described offset cancellation (and flicker noise reduction) techniques can be implemented with a huge variety of different circuits. Due to the importance of this subject, the research activity on offset cancellation techniques is still intense, leading to an ever-growing number of different architectures. In this paragraph, we will limit to very basic circuits. We will start from a time continuous instrumentation amplifier and we will apply the various techniques to it in order to cancel its offset and low frequency noise.

Fig.1.17 shows a method that can be used to apply AZ or CDS to the amplifier *A*. The numbers close to the switches (1 or 2) indicate the phase where they are closed.

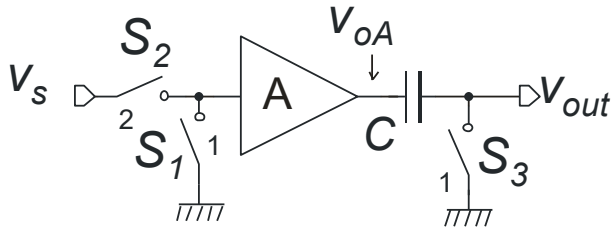


Fig. 1.17. Simple implementation of the auto-zero technique

The configurations of the circuit in the two phases are shown in Fig.1.18. In the first phase the amplifier input is shorted to *gnd*, so that, considering Eq.(1.1), the amplifier output signal $V_{oA}$ is equal to $-Av_n^{(1)}$, where $v_n$ is the input voltage error, including noise and offset, and the superscript (1) means that this signal refer to phase 1. Since $V_{out}$ is also shorted to ground, the $V_{oA}$ value is stored into capacitor C.

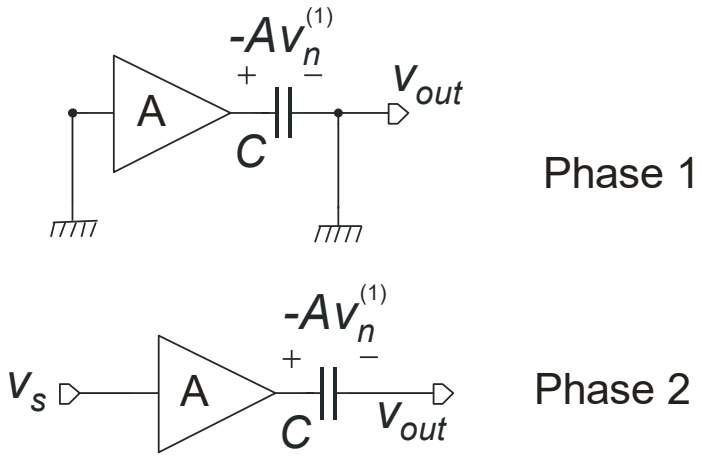


Fig. 1.18. Signals in the two phases of the circuit in Fig.1.17.

In phase 2 the amplifier is connected to the input signal and the output voltage $V_{out}$ is given by:

$$v_{out}^{(2)} = A\left(v_s(t) - v_n(t)\right) - \left(-Av_n^{(1)}\right) = A\left[v_s(t) - \left(v_n(t) - v_n^{(1)}\right)\right] \tag{1.27}$$

During the whole phase 2 the circuit behaves like a time continuous amplifier with an effective input noise given by $v_n(t) - v_n^{(1)}$. Considering that phase 1 and 2 are the AZ and normal operation phases, respectively, and noting that $v_n^{(1)}$ is the noise voltage sampled at the end of phase 1, we conclude that Eq.(1.27) is equivalent to Eq.(1.2), proving that the circuit of Fig.1.17 actually performs the auto-zero procedure.

CDS can be also obtained with the circuit of Fig.1.17, by simply adding a block that samples $V_{out}$ at the end of phase 2. In this case, Eq.(1.27) becomes:

$$v_{out}^{(2)} = A\left[v_s^{(2)} - \left(v_n^{(2)} - v_n^{(1)}\right)\right] \tag{1.28}$$

where the superscript (2) indicates a quantity sampled at the end of phase 2. Since $v_n^{(1)}$ is sampled at the end of phase 1, Eq. (1.28) clearly represents CDS operation.

Possible timing for the clock that controls the switches is shown in Fig.1.19, where phase 1 and 2 are coded by a clock state of 0 and 1, respectively. Note that, in the case of AZ, it is necessary that phase 1 (i.e. the AZ phase) lasts much less than phase 2. On the contrary, this restriction does not apply to the CDS, in which phase 1 and 2 may have similar duration. CDS also requires the output signal to be sampled at the end of phase 2, as indicated in the figure. Sampling can be followed by analog-to-digital conversion, producing a discrete time signal or by a circuit that keep the sampled value constant until the next sample producing a “piece-wise constant” time continuous signal (sample and hold).

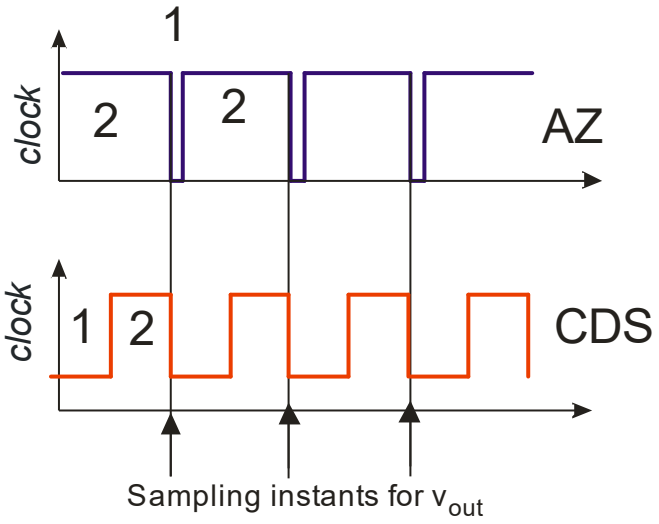


Fig. 1.19. Clock signals for the circuit in Fig.1.17 implementing AZ (top) and CDS (bottom)

The scheme of a simple chopper amplifier is shown in Fig.1.20. Both the modulator and demodulator are implemented with a switch matrix called "chopper modulator". Considering the modulator at the amplifier input, we observe that in phase 1 $v_{in}=v_s$, while in phase 2, $v_{in}=-v_s$. This is equivalent to multiplying $v_s$ by the waveform $m(t)$, assuming that $m(t)$ is 1 in phase 1 and –1 in phase 2. Similarly, the demodulator, which is identical to the modulator, multiplies the amplifier output signal by $m(t)$. Therefore, the circuit of Fig.1.20 is equivalent to the block diagram of Fig.1.11. The advantage of this circuit is that the modulator and demodulator are composed only by switches, which can be easily implemented with pass transistors or pass-gates in CMOS technology. Note that the structure of the chopper modulators requires the signals to be differential. Since this requirement applies to both the input and output of the amplifier, fully-differential architectures are necessary. Single-ended architectures are also possible but they are based on different switch/amplifier configurations that exhibit poorer performances.

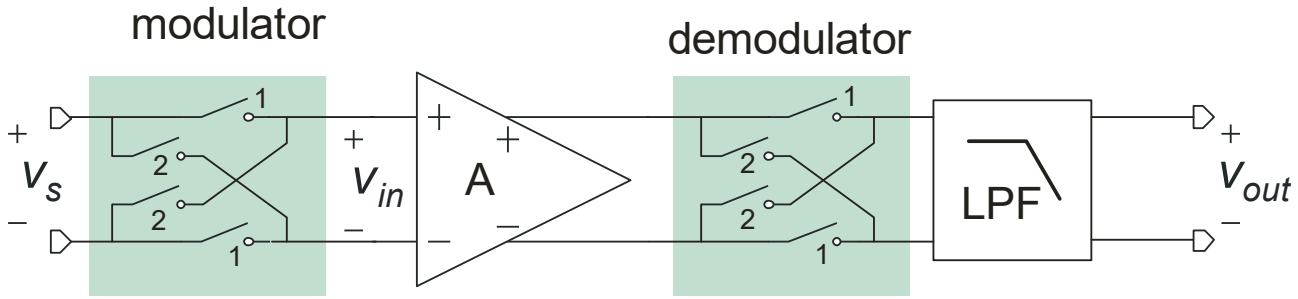


Fig. 1.20. Simplified block diagram of a chopper amplifier

## 1.6 Comparison between AZ, CDS and CHS. .

First, it should be observed that, in practical use, there is a certain degree of confusion among these terms. Indeed, AZ is often used to indicate also CDS, since, as we have seen, CDS can be obtained by properly sampling the output of an AZ amplifier. Furthermore, the term "chopper" is used also for AZ and CDS, since it was inspired by the operation of the switches that, with their continuous opening and closing, seem to be "chopping" the signal. This impression was enforced by early chopper amplifiers (developed in late '40s), which used electromechanical switches (relays), whose operation resembled the movement of a cutting tool, such as an axe. Since all the tree techniques use switches, they are often incorrectly referred to as "chopper". This confusion even involves datasheets and technical notes of integrated circuits.

In spite of this, it is important to keep these techniques well distinguished, since they have peculiar characteristics that should be kept in mind when choosing which one is optimal for a particular application. The main characteristics of the three techniques are summarized in Table 1.1.

| Method | Signal bandwidth ($B_S$) | Residual baseband noise ($f<f_{ck}/2$) | $f_{ck}$ constraints | Particular characteristics |
|---|---|---|---|---|
| AZ | $B_S=B$ | $\frac{2B}{f_{ck}}S_{BB}$ | $f_{ck}<<B$ | Maintains the original time continuous frequency response of the amplifier. |
| CDS | $B_S<f_{ck}/2$ | $\frac{4B}{f_{ck}}S_{BB}$ | $f_{ck}<B/3$ | Fully sampled data system. |
| CHS | $B_S<f_{ck}$ | $S_{BB}$ | $f_{ck}+B_S<B$ | Requires fully-differential architecture and the presence of an effective low pass filter. |

Table 1.1. Characteristics of the three techniques compared

Many of these characteristics have been already discussed in previous paragraphs. The limitations on the signal bandwidth imposed by the CDS technique are simply due to the fact that also the signal is sampled, so that $B_S<f_{ck}/2$ to avoid signal aliasing. In the case of chopper amplifiers, the $B_S$ limit is imposed by the LPF, whose upper band limit should be lower than the clock frequency, to reject the offset and flicker noise shifted at higher frequencies by the demodulator. Considerations about the filter implementation indicate that in practical cases $B_S<<f_{ck}$.

As far as the frequency constraints are concerned, we have to observe that an amplifier responds to an input step in a time that is roughly equal to $1/B$. In AZ and CDS circuits, the amplifier input is shifted from zero (phase 1) to the input signal (phase 2) and back in any clock cycle. For correct operation, it is necessary that the amplifier have enough time to settle to the final value after each commutation. In

AZ, the critical phase is phase 1, since it is the shorter one. Since the settling time is roughly equal to $1/B$, we can write for AZ:

$$\frac{1}{B} < t_{AZ} << T \tag{1.29}$$

Since $T=1/f_{ck}$, we can easily obtain that $f_{ck}$ should be much lower than the amplifier bandwidth.

In the case of CDS, the two phases can be of the same duration. Therefore, the amplifier settling time should be shorter than $T/2$. Thus, we have to impose: $1/B<T/2$, which leads to $f_{ck}<2B$. This is a theoretical limit. We have indicated $f_{ck}<3B$ in Table 1.1 to allow a greater margin, as derived by common practice.

In the case of chopper amplifiers, the limitation indicated in Table 1.1 is due to the fact the amplifier bandwidth should include at least the first replica of the input signals produced by the modulator.

Finally, we will consider the residual noise in the base-band region. In this respect, the solution that performs better is the CHS amplifier, since it does not suffer from noise fold-over phenomena, so that the residual noise density is simply $S_{BB}$. In the case of AZ and CDS, it could seem that the CDS residual noise density is twice that of AZ. However, for the limitation of the clock frequency, $B/f_{ck}$ is much greater than one (up to 1000) in AZ while it can be as small as 3 in CDS. For these reasons, the residual noise density is generally much higher in AZ than in CDS.

This limitation of the AZ amplifier can be circumvented using a so-called "ping-pong" architecture[2]. A simplified representation of a ping-pong AZ amplifier is shown in Fig.1.21.

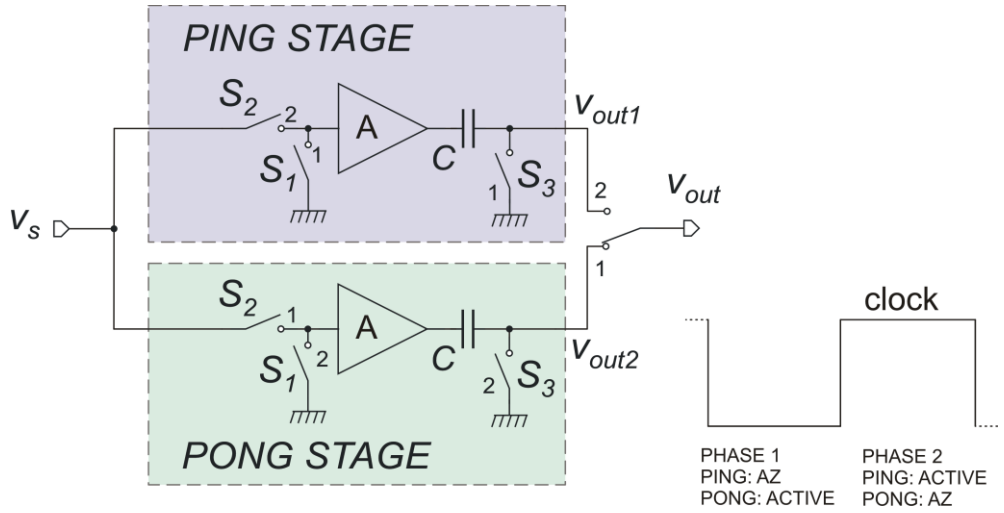


Fig. 1.21. Principle of operation of the ping-pong auto-zero amplifier

In practice, the circuit is formed by two nominally identical structures, indicated as "ping" stage and "pong" stage. Each stage is a complete AZ amplifier. The ping and pong stages are clocked in a complementary way, so that when the ping stage is in the auto-zero phase, the pong stage is active (i.e.

it amplifies the signal) and vice versa. In this way, each stage can spend much more time in the AZ phase (up to $T/2$), since the signal is handled by the other stage and a continuous-time path from the input to the output is provided in the whole clock period. With the ping-pong architecture, the AZ amplifiers do not need to respect condition (1.28), so that the bandwidth and clock frequency are subject to the same (more relaxed) limitations as the CDS

In conclusion, AZ techniques are to be preferred if we want to obtain an amplifier that can be used as a normal time-continuous circuit. AZ is particularly suitable for operational amplifiers since the original frequency response is maintained and the amplifier can be used in closed loop application with unaltered phase margin. This is paid with a relatively large baseband noise density. A better noise performance can be obtained by using ping-pong architectures, which, on the other hand, need duplication of the AZ stage, resulting in greater silicon area occupation and power consumption.

CDS offers a better noise performance but it is a sampled data approach. This is the technique to be preferred when the input signal is already sampled, as it happens in switched capacitor circuits. If we apply the CDS technique to a time-continuous amplifier, designed to read a time continuous signal, we should be aware that the circuit does not sample only the signal but also the noise of the source (e.g. thermal noise associated to the source resistance). Even in the case that the signal is band-limited for its nature, an anti-aliasing filter is necessary to limit the noise bandwidth, which, otherwise, would be aliased and replicated several times in the base-band.

Finally, CHS is by far the most effective technique in terms of residual noise. On the down side, it imposes similar restrictions to the signal bandwidth as the CDS, since it deeply changes the original amplifier frequency response, mainly due to the required output LP filter. In addition, fully-differential architectures are recommended for the implementation of chopper modulation amplifiers, resulting in increased topological complexity. Another important drawback of chopper amplifiers is that implementation of the LPF using only integrated components (capacitors and resistors) is challenging and involves large silicon area occupation.

**References**

[1] C. C. Enz and G. C. Temes, “Circuit techniques for reducing the effects of op-amp imperfections: Autozeroing, correlated double sampling and chopper stabilization,”Proc. IEEE, vol. 84, no. 11, pp. 1584–1614, Nov. 1996.

[2] M. A. P. Pertijs and W. J. Kindt, “A 140 dB-CMRR Current-Feedback Instrumentation Amplifier Employing Ping-Pong Auto-Zeroing and Chopping”, IEEE J. Solid State Circuits, vol.45, no. 10, pp. 2044-2056, Oct. 2010.